Article: Restoration by other Means: CT Scanning and 3D Computer Modeling for the re-Restoration of a Previously Restored Skull from the Magdalenian Era
Author(s): J. P. Brown, Robert D. Martin
Source: *Objects Specialty Group Postprints, Volume Twenty-One, 2014*
Pages: 81-101
Editor: Suzanne Davis, with Kari Dodson and Emily Hamilton
ISSN (print version) 2169-379X
ISSN (online version) 2169-1290

RESTORATION BY OTHER MEANS: CT SCANNING AND 3D COMPUTER MODELING FOR THE RE-RESTORATION OF A PREVIOUSLY RESTORED SKULL FROM THE MAGDALENIAN ERA

J. P. BROWN, ROBERT D. MARTIN

ABSTRACT

The Cap Blanc skeleton was discovered in France in 1911 by a workman who struck the skull at least once with a pickaxe while lowering the floor of the recently excavated rock shelter at Cap Blanc. The skeleton proved to be a Magdalenian era human and was subsequently acquired by the Field Museum in 1927. It was initially displayed with the fragmentary skull, but, in the early 1930s, the skull was reconstructed under the direction of Dr. Gerhardt von Bonin of the University of Illinois.

In 2012, we were able to use a mobile CT scanner to image the bones of the skeleton, including the skull. Upon examination of the scans, it became apparent that some features of the reconstruction of the cranium (sloped brow, small orbital cavities, and projecting nasal bones with large nasal opening) were anatomically incorrect, perhaps due to a self-consciously primitive restoration of the skull. We briefly considered reversing the 1930s reconstruction and using the original skull fragments to produce a more anatomically realistic reconstruction, but the importance of the specimen and the robust nature of the adhesive and gap-fill used in the 1930s reconstruction made the risk of damage while reversing the restoration unacceptably high. We, therefore, attempted to restore the skull to a more anatomically feasible state by converting the CT scan to a 3D software model showing each fragment in its current alignment, and then repositioning the fragments in software to produce a new reconstruction which could be viewed in software. We then 3D-printed the new reconstruction for further study.

In this paper we discuss the methods and software used for extracting and repositioning the fragments and the problem of arriving at a definitive reconstruction by this method. We include some commentary on 3D printing as a long-term preservation problem with consideration on the longevity of 3D-printed artwork. Finally, we review the result of our re-restoration of the skull.

1. INTRODUCTION

From 2006, thanks to the generosity of local hospitals and private companies, x-ray computed tomography (CT) scanning has become part of the methodology of technical examination and documentation of objects and natural history specimens at the Field Museum. Since then we have scanned and analyzed over one hundred objects both large and small. This is not to say that CT scanning has replaced conventional examination by projection x-radiography, but rather that the high dimensional accuracy of CT scans, and the ability to reconstruct the interior of objects in three dimensions, provides essential information for complex objects. This three-dimensional accuracy largely eliminates the geometric distortion and superimposition effects which can be a problem when using conventional projection x-radiographs to examine the interior of objects.

This article briefly outlines the acquisition of x-ray CT data using medical gantry CT scanners, how this data can be processed to show useful information about the interior of complex museum collection items, and how 3D polygon models can be extracted from the CT data for further work. It shows how CT-derived 3D models of the fragments of a previously restored prehistoric human skeleton were used to produce a new, and more anatomically feasible, reconstruction of the skull.

2. CT SCANNING

2.1 ACQUIRING CT DATASETS

There are two stages in generating CT scan data: the first is scanning and the second is mathematical reconstruction. In practice, particularly where helical scanning is used on modern medical CT scanners, these activities may proceed approximately in parallel.

In the scanning phase, a large number of projection x-ray images are taken around a single axis of rotation to give 360° imaging of an object. In a third-generation medical gantry CT scanner (the most commonly encountered type), scanning is achieved with an x-ray source and x-ray detector mounted on opposite sides of a steel ring housed in the gantry. The object to be scanned is placed prone on a bed with appropriate supports and the bed is raised or lowered so that the axial center of the object is aligned with the axis of rotation of the ring. To acquire projections, the ring spins while the bed moves into the bore of the gantry, carrying the object through the ring, and a fan beam of x-rays is projected from an x-ray source, through the object, to the detector. This method of helical (*spiral*) scanning is our preferred data-acquisition method if 3D rendering or multiplanar reformatting is required.

The projection images acquired from scanning are used as inputs for a mathematical reconstruction of the scanned volume. Multiple different reconstructions can be performed from one set of projections by applying alternative mathematical filters to the same projection data. In medical CT scanning, the mathematical convolution filter (*kernel*) used in reconstruction determines the trade-off between image sharpness and noise: higher spatial resolution and therefore image sharpness implies greater noise; *softer* kernels imply less noise but have lower spatial resolution (Weiss et al. 2011). Medical reconstruction software for a particular make of scanner will come preloaded with a range of proprietary reconstruction kernels, which can be selected to provide the best balance between noise and image sharpness for a particular scanning situation.

The reconstructed data are represented as a 3D grid of x-ray attenuation values. Each non-null value in the matrix is the mean x-ray attenuation calculated for a small, rectangular portion (*voxel*) of the total volume scanned. In medical CT scanning, the matrix is stored as a stack of evenly spaced bitmap images in DICOM (Digital Imaging and Communications in Medicine) format.[1]

2.2 IMAGING CT DATA SETS

2.2.1 Two-Dimensional Imaging

Medical CT data stacks are conventionally viewed axially, slice-by-slice, as a series of 2D grayscale images which are scrolled through in sequence. As an example, consider the Peruvian mummy in a wooden tray (shown prior to rehousing) in figure 1. The mummy was scanned in the tray on a 64-slice GE Medical Systems Lightspeed VCT scanner. Scan settings were 120 kV and 100 mA with 1.2 mm focal spot, 0.625 mm collimation, and a spiral pitch factor of 0.5. The series was reconstructed as 512 × 512 pixel axial slices with 0.7 mm pixel spacing and a thickness of 0.625 mm. These numbers imply that each pixel in the image represents the means x-ray attenuation value of a 0.7 × 0.7 × 0.625 mm portion of the scanned volume. A standard convolution kernel and medium filter were used in the reconstruction.

A single axial slice from the scan, about mid-way through the stack is shown in figure 2a. As in a conventional x-radiograph, whiter areas indicate higher x-ray attenuation values. we can see the layers of textile used in the wrappings, the grain and profile of the wood slats used to create the tray, sections through the mummy's bones (ribs, etc.), the inverted 'U' shape of a section through a gourd vessel

Fig. 1. Peruvian mummy bundle, Chancay culture, ca. 1200 CE, human remains, textile, cordage, ceramic, gourd, cotton boll, seeds, 61 × 42 × 44 cm. (Courtesy of the Field Museum, Department of Anthropology, catalog no. 183925)

inverted above the mummy's chest, and sections through two highly attenuating pottery figurines at right and left.

The reconstruction matrix can be resliced orthogonal to the axial plane to show other views through the series of slices. Figure 2b shows a sagittal slice from the middle of the stack: The role of the inverted gourd vessel in supporting the wrappings above the torso is somewhat clearer in this image. Figure 2c shows a coronal slice through the middle of the stack: The position of the skeleton and the profile of the pottery figurines is made somewhat clearer. The relationship between the axial, sagittal, and coronal planes is shown in figure 2d. Ten years ago such multiplanar reconstruction (MPR) from axial slice data was quite exotic, but nowadays these views can be generated interactively in real time from medical slice data on most desktop computers with freely available software such as ImageJ.

2.2.2 Three-Dimensional Imaging

Three dimensional renderings of CT data can be achieved by mapping the attenuation values in the reconstruction matrix to color and opacity (RGBA) values using a lookup table or transfer function. The structures can be rendered in three dimensions directly from the slice data either by isosurface methods (a particular attenuation value is selected to represent the solid surface, and this value is then rendered as an opaque surface) or by ray-tracing with transparency. These methods work reasonably well on objects where the attenuation values are low at the outside of the object and get higher towards the center, but are less satisfactory where the features near the outside of the object are more attenuating than

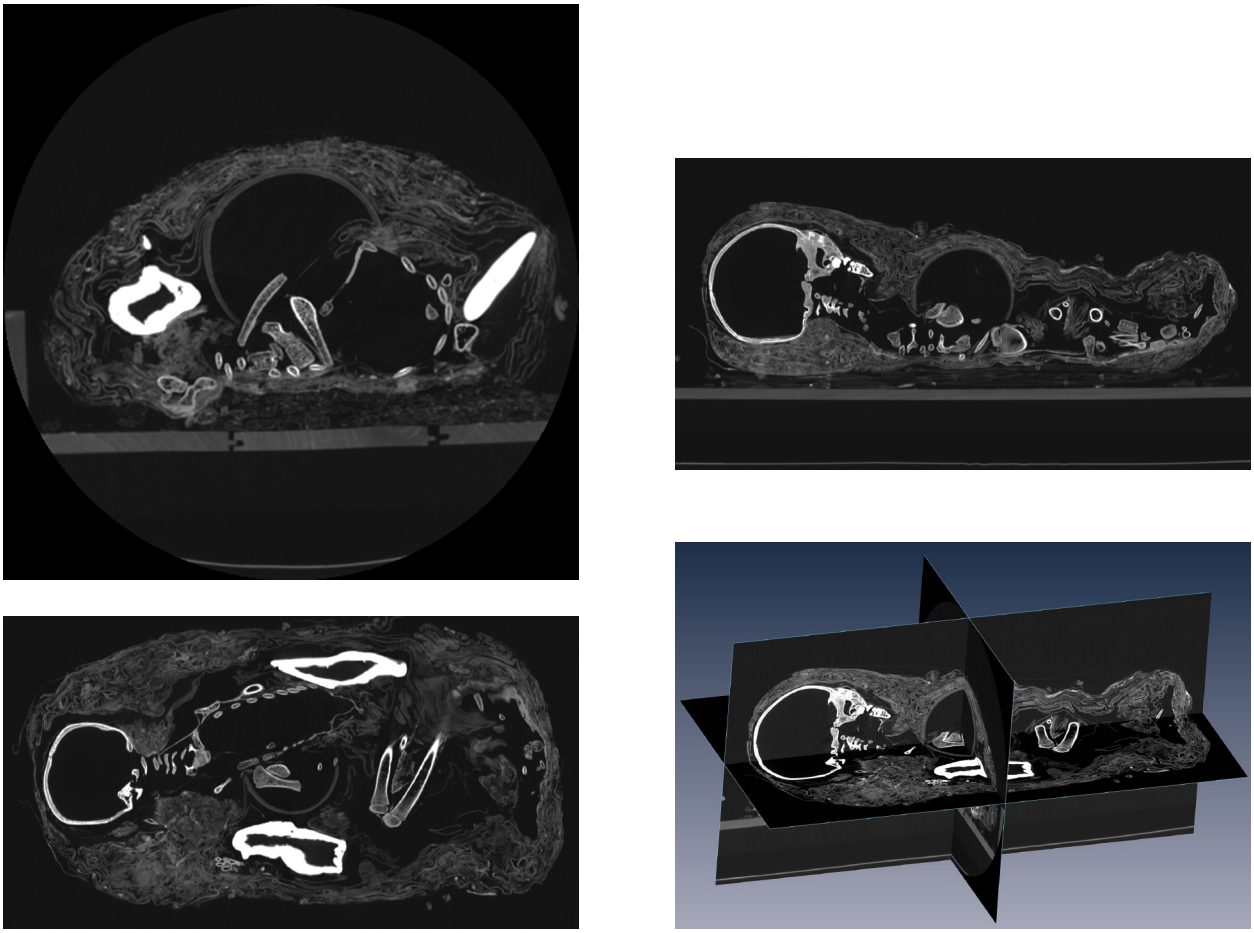

Fig. 2. Two-dimensional views of the reconstructed data set from CT scanning the mummy shown in figure 1: a. axial view at mid-point of the reconstruction matrix, rendered in ImageJ; b. sagittal view at mid-point of reconstruction matrix, rendered in ImageJ; c. coronal view at mid-point of reconstruction matrix, rendered in ImageJ; d. relationship between axial, sagittal and coronal views, rendered in Amira.

the inside, where the surface of a feature inside the object varies significantly in attenuation value, or where different components of the same object have similar attenuation value. For example, figure 3a shows a volumetric rendering of the mummy from figure 2 with a simple linear transfer function to remove the overlying low-attenuation textiles. Although the high-attenuation elements such as bones, teeth, and ceramics show up well, mapping the cloth to a transparent value has also made the (equally low-attenuation) gourd transparent. If the opacity of the low-attenuation values is increased, the cloth reappears and obscures the gourd. Also, while the teeth and the cortical bone of the diaphyses show up well, the spongier bone of the epiphyses and the phalanges are translucent and hard to see clearly.

If applying a single transfer function to the whole reconstruction matrix will not give adequate volumetric rendering, as in the case of the wrappings and the gourd, then segmentation of the data matrix into parts (sometimes called *labeling*) must be performed. Three-dimensional regions of interest (ROIs) are defined on the data and a different transfer function is applied to each ROI. Some ROIs may be made transparent or translucent, others may be made solid, and false color may be applied. ROIs can be defined semi automatically by region growing on the basis of attenuation value: A small sample of voxels that is representative of the region of interest is nominated and then the region is allowed to grow from there so long as the adjacent pixels are within some threshold range close to the attenuation value of

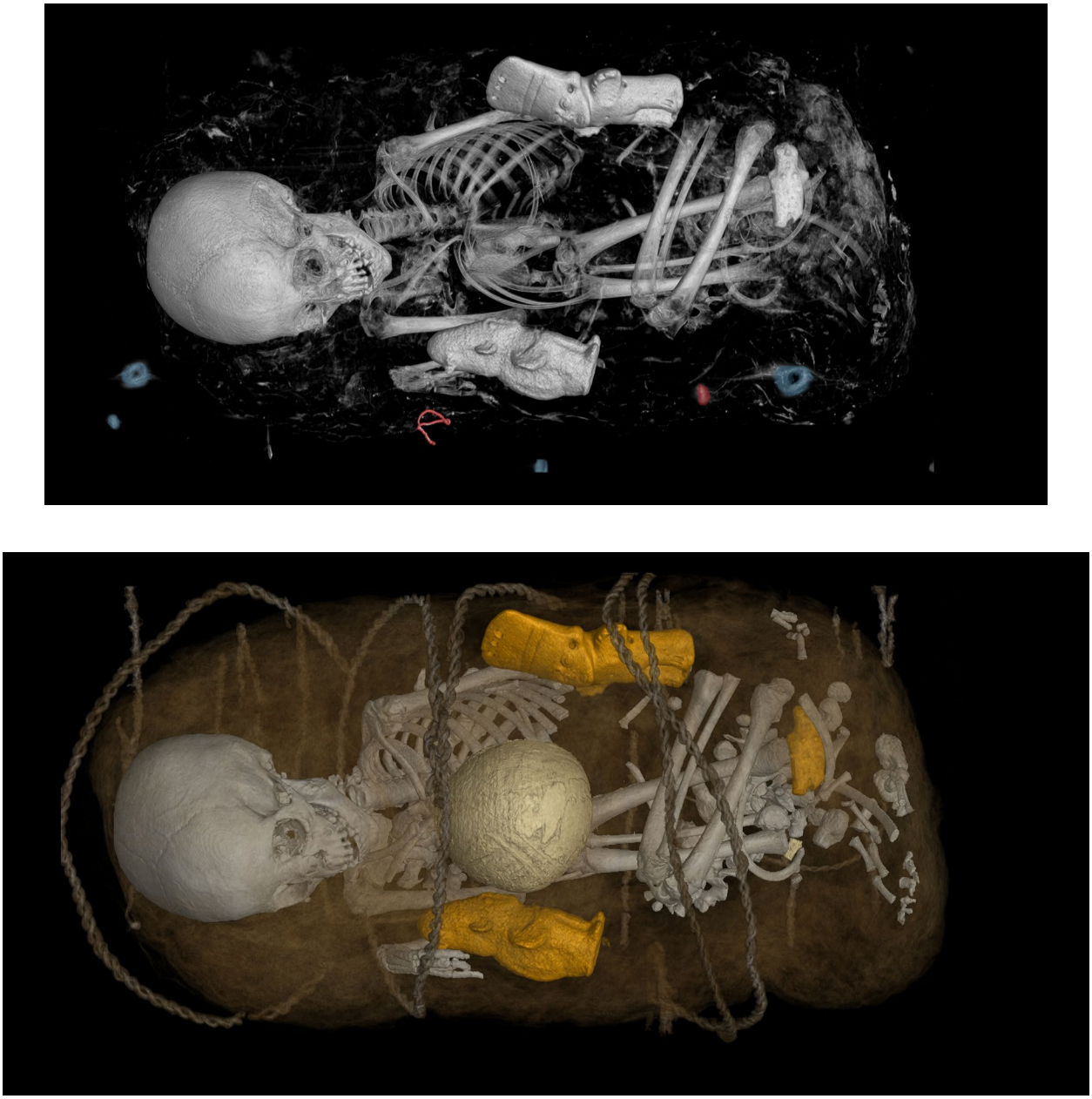

Fig. 3. Three-dimensional views of the reconstructed data set shown in figure 2, rendered in VG Studio Max: a. volumetric rendering with a simple linear transfer function to make overlying wrappings transparent; b. segmentation of the data set allows different transfer functions to be applied to different regions of the data.

the initial sample. Alternatively, when the feature of interest approximates a 3D geometric primitive, the primitive may be outlined on the object to roughly define the region. Some software packages offer Boolean operators that allow the operator to intersect, add, or subtract one or more regions from another, which can make it somewhat easier to refine the region of interest. Where clear attenuation differences between adjacent features of interest are absent, segmentation must usually be performed by manually drawing the profile or outline of the feature on each slice in which it appears. Some segmentation packages offer an interpolation mode which allows outlining the profile on only some of the slices and then allow the software to guess the remainder.

Figure 3b shows the segmented data for the mummy from figure 1; ROIs were defined for the rope, wrappings, wood tray, skeletal elements, ceramics, and the gourd. The wood tray ROI has been made transparent, and the color and translucency of the other regions has been varied independently.

Free software packages for 3D segmentation and rendering include Osirix, Drishti, Voreen, and ImageVis3D. In general these packages work reasonably well on small data sets (< 0.25 GB, about 500 512 × 1512 CT slices) but less well on large data sets (> 1 GB). Commercial packages for handling large data sets include Amira, VG Studio Max, and Mimics. Given adequate hardware, these packages perform well on large data sets, but are expensive, costing from $4,000 to more than $15,000 even after academic discount.

2.3 EXTRACTING POLYGON MESHES

Once a region of interest has been defined, it becomes possible to generate a polygon mesh that approximates its surface in three dimensions.[2] The mesh can then be saved in a suitable digital file format and refined and rendered independently of the CT volume.

To get good polygon meshes from CT data, we need voxels that are as near as possible isotropic; that is, the pixel spacing on the slice images should be as close as possible to the spacing between slices. It is also desirable to have as much detail as possible, so increasing the number of pixels per slice and decreasing the thickness of the slices naturally improve the quality of the resulting mesh. Increasing the resolution of the slices and decreasing slice thickness not only increases the amount of data to be handled (which implies more expensive hardware and software for processing), but also increases the noise on the slice images.

Small-feature contrast improves linearly with decreased slice thickness, whereas noise increases as the square root of slice thickness ratio (Nagel 2004, 24). Essentially, taking thinner slices improves the visibility of small details despite increased noise.

Fig. 4. Polygon meshes of the three ceramic figurines in the mummy bundle shown in figure 3. Meshes were extracted with VG Studio Max, saved to disk, and then rendered in Blender.

On medical systems, the increase in noise down to around 0.5 mm slice thickness can usually be dealt with by choosing an off-the-shelf scanning protocol. As slice thickness is reduced to 0.2 mm (the current limit for medical gantry scanners), setting aside a significant amount of time to optimize the scanning technique and fine-tune the reconstruction parameters for the particular object under examination becomes important if results are to be usable.

Space does not permit a full discussion of optimization of medical CT scanning protocol, but Prokop (2003) provides an accessible summary from a medical perspective. The most important differences between scanning human beings and scanning objects of cultural heritage are the medical necessity to reduce x-ray exposure as far as reasonably achievable (essential for living specimens), and the concern to take scans as quickly as possible to prevent patient movement during the scan. Both of these problems can usually be ignored when CT scanning cultural objects: The ring rotation speed, bed speed, and spiral pitch can all be reduced, and the current to the x-ray source can be increased. All these settings increase the time of the scan and the x-ray exposure, but reduce noise. In practice, the reduction in noise that can be achieved is limited by the ability of the x-ray tube to sustain high output during the extended scanning period.

2.4 PHYSICAL REALIZATION OF POLYGON MESHES

Given a suitable polygon mesh, it is possible to produce a physical copy of the mesh using manufacture that is additive (3D printing) or subtractive (computer numeric control [CNC] cutting); however, a caveat must be inserted here. Although all the segmentation software mentioned earlier can produce good polygon meshes for rendering, a mesh often needs significant modifications to be actually manufacturable. Such modifications include ensuring a manifold surface, removing noise meshes, and repairing self-intersections.

The requirement for a manifold surface can be difficult to achieve by hand. Noise meshes are sometimes discrete *bubbles* located inside the main mesh, other times they are nonplanar mesh faces (those which do not share all their edges with adjacent faces, but stick out on their own). The bubble meshes are not usually anchored to the main surface, but can complicate printing and are usually best removed. Nonplanar faces and self-intersections usually result in an unprintable mesh. Resolving these imperfections requires additional software directed towards 3D printing or CNC cutting. At present, we have found only one free software package that is reasonably satisfactory for preparing polygon meshes for additive manufacture: MeshMixer. Commercial packages directed toward producing manufacturable objects from polygon meshes (Geomagic, Magics, and 3-matic) are relatively expensive and have a fairly steep learning curve. Often, it is easier to pay a local 3D printing service to refine the mesh to manufacturability, or there may be a local MakerSpace that can assist.

2.4.1 Additive Manufacture

In additive manufacture, the solid is built up from thin layers of material, each layer deposited on the previous one (Gibson et al. 2010). Techniques for additive manufacture include extrusion of thin layers of molten polymer, which is allowed to harden (fused deposition modeling [FDM]), selective laser sintering (SLS) of powdered metals or polymers and stereolithography (SLA) with UV-cured resins.

Figure 5 shows an example of an additively manufactured copy of one of the ceramic figurines, printed from a polygon mesh derived from the CT data shown in figure 3. What is particularly exciting about this is the possibility of nondestructively imaging features inside an object and then producing a physical copy for study. There is a wide variety of materials—metals and polymers—that can be used, and, with appropriate software, it is possible to find a technique that will print most shapes. Current disadvantages of additive manufacture are that production is quite slow (one vertical inch per hour is

Fig. 5. 3D print of the polygon mesh of the center figurine from figure 4. The mesh was extracted using VG Studio Max, refined in 3-matic and printed in white polylactic acid on an FDM machine.

considered fast), the build volumes are limited (18 × 12 × 8 in. is considered a large build volume), and machines are optimized for a particular, narrow range of output materials.

Printing in metals is prohibitively expensive for large volumes. Printing in polymers is more affordable, but unfortunately many of the polymer materials perform poorly in Oddy tests. The tests we have performed on FDM and SLA materials, although by no means exhaustive, have given results equivalent to the unusable and temporary criteria described by Schiro (2011).

This finding has important implications for the collection of 3D-printed art and the use of 3D-printed materials in museum exhibits. The general attitude of 3D-printer suppliers seems to be that, given the polygon mesh, we can always print another one. This is true up to a point, but there is considerable variation in the surface finish of 3D-printed objects, particularly when manufactured on hobbyist FDM and SLA machines. If an artwork is manufactured on a particular kind of machine with a particular brand of output material, there is no guarantee that the surface finish of the resulting piece will be replicable 20 or 30 years from now. This problem is somewhat parallel to that encountered in computer-based installation art. As technology changes, realizing the original artistic intent from a digital original can become difficult or impossible.

The most satisfactory additive production method we have found so far is laser sintering using nylon powder. We find no reaction on the Oddy test, and parts made with this technique are robust, relatively inexpensive, and take paint well.

2.4.2 Subtractive Manufacture

Subtractive manufacture is faster and has larger build areas than additive manufacture; machines to process 4 × 8 ft. stock are readily available. In the simplest set-up—a three-axis CNC machine—a

computer-controlled milling head moves over a sheet of material, progressively cutting away excess stock to leave the required shape behind. A wide range of conservation-safe materials can be machined to shape by this method, but the build height is limited and undercuts are a problem. If the object to be manufactured has significant thickness, it is usual to divide the model into multiple sections of an appropriate depth, machine these individually, and then assemble the parts.

This workflow of CT scanning, segmentation, 3D modeling, and 3D printing brings us to the reconstruction of the previously restored skull of the Cap Blanc skeleton at the Field Museum.

3. HISTORY OF THE CAP BLANC SKELETON

3.1 DISCOVERY AND EARLY TREATMENT

The early human skeleton familiarly known as the Cap Blanc skeleton, more recently as Magdalenian Girl, and more recently still as Magdalenian Woman, was discovered in France in 1911. The discovery occurred while a protective structure was being built around the mouth of the Abri du Cap Blanc, a recently excavated rock shelter with a large (15 × 3 m) and important prehistoric carved frieze of running horses and bison on its back wall (Bourdier et al. 2010). Part of the planned work involved lowering the floor level inside the shelter to permit a better view of the carvings. During the digging, one of the workmen discovered the skeleton after striking it with a pickaxe, breaking the skull. Two specialists, Capitan and Peyrony, were dispatched from Paris to assess the skeleton and found that the blow had broken the cranium, but that the rest of the skeleton was reasonably complete (Capitan 1911). The skeleton was block-lifted and, after some delay, transported to Paris for treatment at the *Laboratoire de Paléontologie* of the *Muséum National d'Histoire Naturelle* (MNHN). A receipt for Fr. 180 for the restoration of the skeleton, written to M. Grimaud, the owner of the rock shelter, by Capitan shows that the treatment was either in progress or complete in the summer of 1914 (Capitan 1914).

After treatment was complete, the skeleton was returned to the owner of the Cap Blanc site with a letter from the preparator at the MNHN, J. Papoint (1915). Papoint noted that the damaged skull could not be fully reconstructed and was being returned in two blocks, one of which comprised the upper and lower jaws and the cervical vertebrae. Papoint did not detail the contents of the other block, but it seems reasonable to presume that it contained whatever had been recovered of the cranial vault. He also noted that the two blocks were "very fragile and should be unpacked with care."

3.2 ACQUISITION BY THE FIELD MUSEUM

At some point between 1915 and 1924, the skeleton was shipped to the American Museum of Natural History in New York (AMNH) so that it could be evaluated for purchase.

The AMNH ultimately declined to purchase the skeleton and, in 1927, the skeleton was acquired by the Field Museum. Concerned about shipping such a fragile specimen, the AMNH, with the assent of the Field Museum, consolidated the skeleton with Ambroid, a recently developed cellulose nitrate cement.

The first detailed photograph we have of the skeleton shows it on display in 1927 (fig. 6). The skeleton appears much as described by Papoint, except that the skull is now in six pieces. Of the two blocks mentioned in 1915, the block comprising the jaws and cervical vertebrae appears to be intact, but the block that presumably contained the cranial vault has separated into at least five pieces. A letter immediately before the acquisition of the skeleton describes the skeleton as "intact, except for the fact that the skull is in several pieces"(Nicoll 1926), so it is possible that damage occurred before shipment to the Field Museum.

Fig. 6. The Cap Blanc skeleton on display in the Field Museum in 1927: a. overall view; b. detail of the fragments of the skull. The skeleton dates to 13,000 to 11,000 BCE (Courtesy of The Field Museum, CSA55472. Department of Anthropology, catalog no. 42943)

3.3 PRE-WORLD WAR II RECONSTRUCTION OF THE SKULL FRAGMENTS

In 1932, the skeleton was taken off display so that the skull could be restored by Mr. T. Ito under the direction of Dr. Gerhardt von Bonin, a medical anthropologist at the University of Illinois at Chicago (Field 1938). von Bonin subsequently published an analysis of the skeleton (1935) in which he briefly described seven pieces of the skull before reassembly, the seventh resulting from cleaning and separating the block containing the upper and lower jaws. Later in the publication, he described the reconstruction of the skull and mentioned that the joint between the rim of the left orbit and the frontal bone was "somewhat worn down so that the position of this piece could not be ascertained with perfect accuracy" (1935, 20). The skull fragments were readhered and the areas of loss (particularly the nasal region and the proper right half of the cranial vault) were gap-filled with plaster, most of which was then painted black,

Fig. 7. von Bonin's 1932 reconstruction of the skull fragments shown in figure 6. Human remains with painted dental plaster fill, 21 × 15 × 14 cm. (Courtesy of The Field Museum, CSA77605. Department of Anthropology, catalog no. 42943)

while the upper half of the interior of the cranial vault was coated with multiple applications of plaster. The final result of the reconstruction is shown in figure 7.

3.4 RECENT WORK

In 2004, the skeleton was taken off display for transfer to new exhibit, and we were able to perform projection x-radiography on the bones. As evident from figure 8, von Bonin's reconstruction

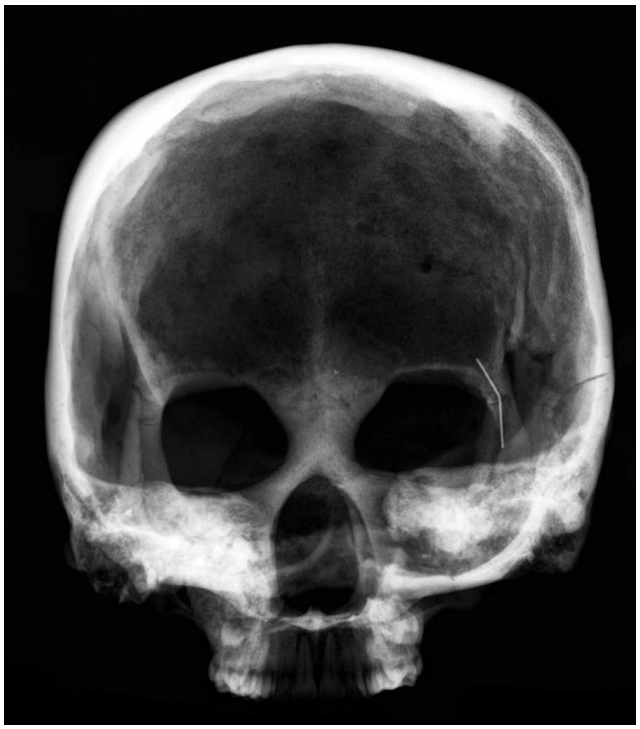

Fig. 8. Digital x-radiograph of the cranium of the Cap Blanc Skeleton, Dec 10, 2004.

Fig. 9. Magdalenian skeleton on display in the Evolving Planet exhibit, 2006. Courtesy of William Pestle.

included an undocumented metal pin to hold the rim of the left orbit in place. The skeleton was placed back on display in the new Evolving Planet exhibit in 2006 (fig. 9).

4. PRODUCING A NEW RECONSTRUCTION OF THE SKULL

4.1 CT SCAN

In 2012, the skeleton was taken off display before its appearance in an exhibit devoted to the Lascaux cave paintings, and we were able to x-ray CT scan all the bones. The condition of the skull at this time is shown in figure 10. There is some loss of paint from the plaster fill, and unpainted fills are apparent at the joint between the left orbital margin and the frontal bone and at the front of the upper jaw.

Two scans were conducted on a 64-slice GE Medical Systems Lightspeed VCT scanner mounted in a mobile trailer and positioned in the museum's parking lot. The first scan was taken at 140 kV, 94 mA, and the second at 120 kV, 100 mA, both with 0.7 mm focal spot, 0.625 mm collimation, and a spiral pitch factor of 0.5. The data were reconstructed as 512 × 512 slices with 0.48 mm pixel spacing and

Fig. 10. Condition of the cranium of the Cap Blanc skeleton in 2012. Courtesy of J.P. Brown.

0.625 mm slice thickness, the higher kV scan using a bone kernel and the lower-kilovolt scan using a convolution kernel, both with a medium filter.

On examination of the scans, it seemed to us that the restoration provided a self-consciously *primitive* reconstruction of the skull's appearance. In particular, the low, backward-sloping brow and the narrow orbital cavities did not seem anatomically modern even though the C14 dates for the skeleton would indicate that an anatomically modern reconstruction would be appropriate. The essential feature that gave von Bonin's reconstruction this primitive appearance was the positioning of the maxilla relative to the frontal bone, and the main evidence for the position chosen by von Bonin was the link, albeit floating, formed between the two pieces by the fragmentary proper left zygomatic bone.

We briefly discussed reversing the 1930s reconstruction and using the original fragments to produce a new and more anatomically realistic reconstruction; however, the importance of the specimen and the extensive nature of the restoration (including the embedded metal pin) made the risks of reversing the restoration quite high. We decided instead to try to create a virtual 3D model of each of the fragments in their current alignment and then reposition the fragments in software to produce a new, virtual, restoration.

4.2 SEGMENTATION

The x-ray attenuation of the plaster fill (calcium sulfate) was sufficiently similar to the attenuation of cortical bone (calcium hydroxyapatite) that automatic segmentation produced unsatisfactory results. The large area of plaster reconstruction at the right of the skull could be easily selected using 3D lasso tools and Boolean operations, but the segmentation of plaster from bone where the two materials joined had to be conducted by eye, almost slice-by-slice in some regions. Where plaster met the trabecular bone of the skull, this was not too difficult. The plaster is relatively homogenous and has a very different texture from the spongy interior bone. Where the plaster met the outer cortical bone of the skull, distinguishing between plaster and fill could be quite difficult. We used VG Studio Max to divide most of the plaster from the bone, taking about three days to achieve a satisfactory result (fig. 11).

Fig. 11. Segmentation of the bone and fill on the skull of the Cap Blanc skeleton; the regions of fill are colored amber. Rendered in VG Studio Max.

4.3 MAKING POLYGON MESHES OF THE FRAGMENTS

Having divided the bone from the plaster, we then needed to segment out the individual fragments of bone and make polygon meshes of them. This task proved extremely difficult in VG Studio Max and, in the end, we transferred the problem to the Mimics software package and produced polygon meshes in the 3-matic package that accompanies Mimics (fig. 12). Even so, it took over two weeks to get close to a good representation of the fragments, primarily because we found that the skull was far more fragmentary than we had suspected. In all, we identified 36 fragments (not counting loose teeth). On the basis of the previous reading of the history of the skeleton, we had expected to be looking for seven or eight fragments. The additional fragmentation of, for instance, the left parietal bone of the cranium is fairly obvious in figure 10, but this was not apparent before removing the skeleton from display because, as figure 9 shows, the skeleton was displayed in a crouched position with the skull lying with its left side down.

4.4 DIGITAL RESTORATION

The question then became how to arrive at a more satisfactory arrangement of the fragments. Reconstruction of skulls from CT scanned fragments is not new (Zollikofer et al. 1995), but has generally been carried out on objects with six or fewer fragments. More recently, automatic alignment of meshes from fragmentary objects has been achieved (Brown et al. 2008), albeit in wall-paintings, but this method relies on the constraint of a near flat plane (the painting's surface) and good knowledge of the profile of the edges.

One possible option was to 3D print the fragments and then reassemble them manually. There were two principal difficulties with this approach: first, the difficulty of correctly aligning the floating fragments such as the right mastoid-glenoid and the left orbital margin; second, the uncertainty in the profile of the edges of the fragments meant that the principal guide to correct manual alignment—whether fragments are felt to *lock* into position properly or not—would be compromised. We chose to reassemble the fragments in software. The principal advantages were that we did not have to deal with gravity (no need for intricate supports to hold the floating pieces and the narrow bridge in the left parietal while gap fill was setting) and that we could use mirroring to exploit left–right symmetry to check alignment of the fragments on either side of the skull.

After discussing the problem with craniofacial reconstructive surgeon Dr. Pravin Patel and biomedical engineer Dr. Linping Zhao, we determined that the best approach to the reconstruction was to proceed iteratively. Because we had little *a priori* information on the original shape of the skull, each successive step of the virtual reconstruction would need to be determined on the basis of the previous state of the assembly. To reposition the fragments, we used the free software package, Blender, because it

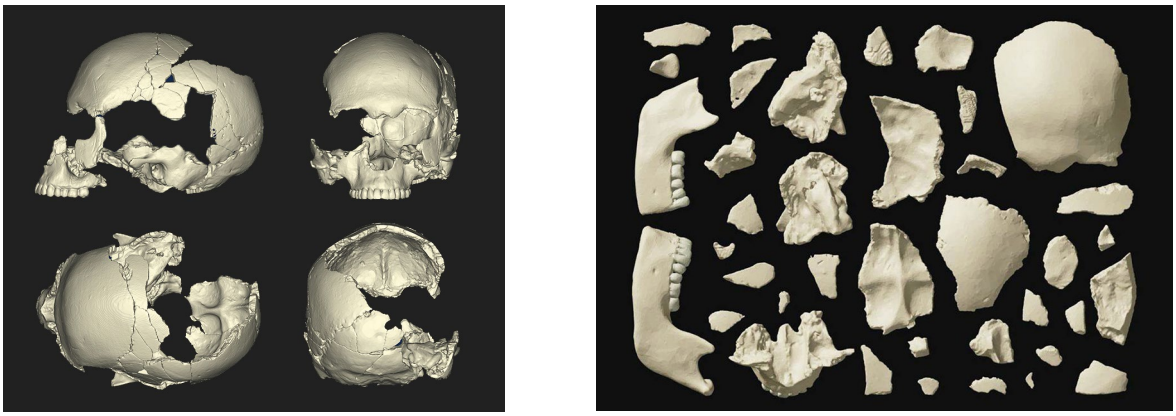

Fig. 12. Polygon models from the segmentation of the bone fragments of the skull of the Cap Blanc Skeleton: a. composite of screen grabs from 3-matic showing the position of the fragment models in von Bonin's reconstruction; b. individual fragments arranged and rendered in Blender.

allows for mirroring, nested parent–child relationships, and can be configured for intuitive interactive repositioning. The parent–child relationship feature was particularly useful in this project. Given the relatively tight joints of von Bonin's reconstruction, we could define groups for each of the 1927 fragments. When the root parent was moved or rotated, all the child fragments would retain their alignment to the parent. Once the position of the group was satisfactory, the positions of the children could be refined individually to give final alignment.

We needed a strong starting point, and we chose to begin with the mandible (lower jaw). As shown in figure 11, the arch of the mandible is broken, just at the proper right of the mid-point. If we could determine the correct alignment of the fragments of the mandible, then we would have a baseline from which to build up the rest of the skull as shown in figure 13. First, we defined a mid-sagittal

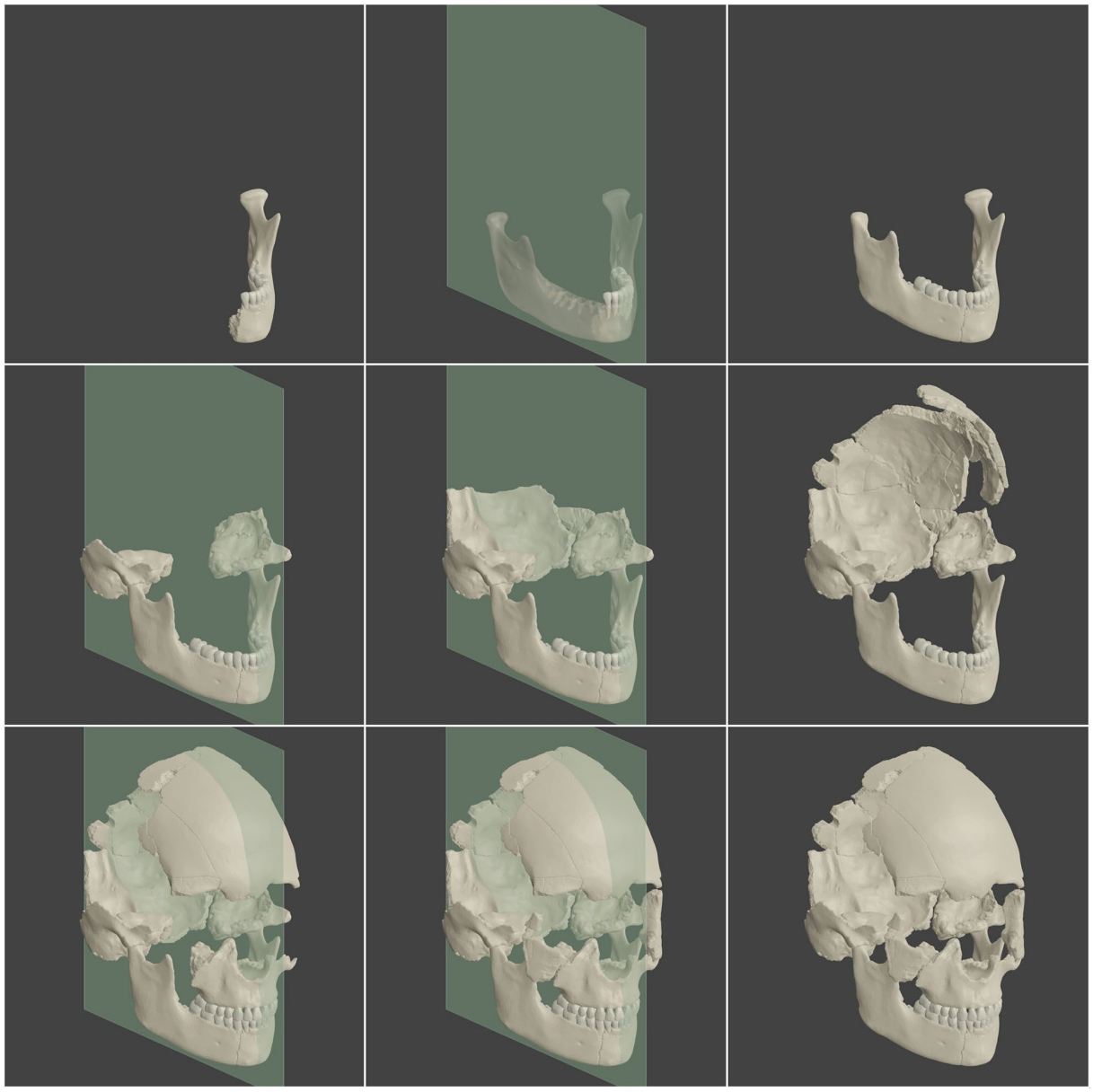

Fig. 13 Process of assembling polygon meshes into a new model of the skull. Top row: aligning the broken fragments of the mandible. Middle row: adding fragments of the temporal, occipital and parietal bones. Bottom row: adding the frontal, mandible, and left orbital arch.

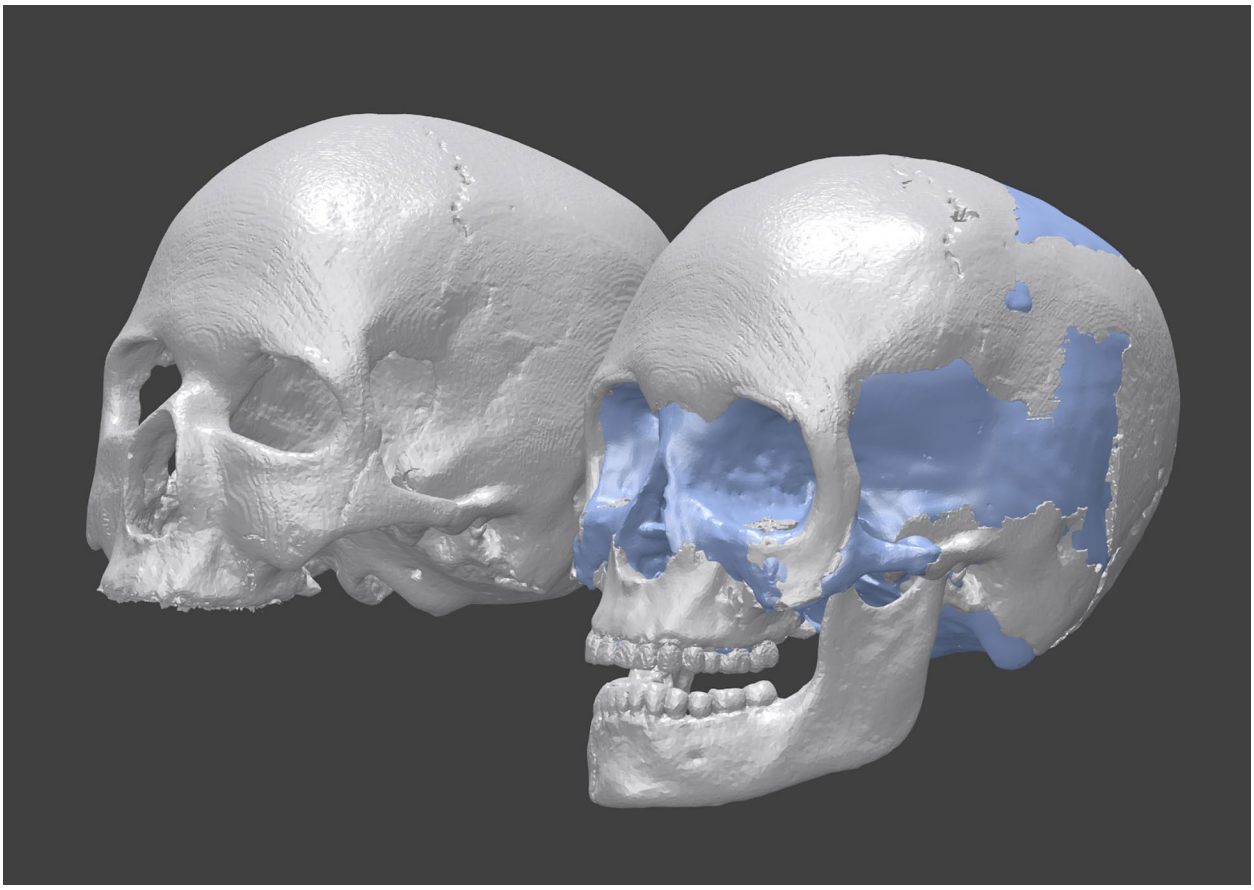

Fig. 14. Comparison of our virtual reconstruction (front) with von Bonin's reconstruction (rear).

mirror plane and then aligned the proper left fragment of the jaw so that, together with its mirror image, we had the appearance of a complete jaw. We then introduced the right-hand fragments and aligned them as best as we could with the mirror image to form the complete jaw. Once the mandible was complete, we were able to align the left and right temporal bones with the condyles of the mandible. We used the mirror plane to check the alignment of the temporal bones with each other until asymmetry was minimized, and this gave us a basis for building the cranium. We could then place the occipital, again using the mirror plane to check alignment. Then we built up the proper left parietal and added the fragments of the frontal, again checking alignment with the mirror plane. Next we added the maxilla, checking the alignment with the teeth of the mandible and with a mirror plane. Finally, we added in the fragment of the left zygomatic arch, again using a mirror plane to check alignment.

The losses on the proper left side of the cranial vault were gap-filled using virtual clay sculpting in Blender and ZBrush, and then the left hemisphere was mirrored across to fill the loss on the proper right side. Figure 14 shows our virtual model in comparison to von Bonin's reconstruction. The resulting model was refined in 3-matic to create a printable solid and then printed off-site using a Stratasys PolyJet printer (fig. 15).

5. CONCLUSIONS

The result of this virtual reconstruction is a physical model that is an anatomically defensible reconstruction of the skull, achieved without risking damage to the original specimen. All steps taken were nondestructive and reversible. The virtual reconstruction is well documented and, in principle, other

Fig. 15. The new reconstruction 3D printed in UV-cured acrylic resin. Courtesy of John Weinstein, courtesy of The Field Museum, A114938d_021B.

interested researchers could proceed through the same sequence of segmentation and virtual reconstruction and compare their result to ours. This ability to repeat or reconsider a virtual restoration is in sharp contrast to hands-on restoration, where detailed documentation and ready reversibility are hard to achieve. On the one hand, the extensive use of the sagittal mirror plane may have made our reconstruction overly symmetrical; on the other, it is not clear how this procedure could be improved, given the loss of original material on the proper right side of the cranium.

One question remains: Why did we identify significantly more fragments than are explicitly mentioned in von Bonin's account of the restoration of the skull? Some of these fragments are clearly present. The matching cracks at the exterior and interior surfaces of the cranial vault can be checked by visual inspection. In the case of some other fragments, the crack is visible at the outside of the skull, but plaster from the von Bonin reconstruction overlying the interior of the cranium prevents visual confirmation of the continuity of the crack at the inside surface. The question of whether some of the fragments that we identified are truly separable pieces of the cranium or whether we have over identified fragments on the basis of stress cracks on the outer surface of the cranium, cracks which do not fully penetrate to the interior surface of the skull vault, could not be resolved at the resolution of the CT scans taken in 2012. We are tackling this question as a new research project and have obtained two sets of higher-resolution scans: 0.2 mm thickness

medical CT scans courtesy of the University of Chicago Hospitals and 0.1 mm isotropic micro-CT scans courtesy of local nondestructive testing company Alloyweld Inspection Co. We are in the process of segmenting these scans to see if we can resolve the question of how much resolution is required in practice to reliably differentiate fragment breaks from nonpenetrating stress cracks.

It should be noted in passing that the process of segmenting the CT scans, generating the mesh models of the fragments, repositioning and mirroring the meshes, gap-filling the resulting model, making it manufacturable, and then producing the printout of the reconstruction was considerably more time-consuming than we had anticipated: at least equivalent to a major object treatment. A nontrivial amount of this time was spent climbing a number of steep learning curves with unfamiliar software, so future work on similar resolution data should proceed significantly faster.

ACKNOWLEDGMENTS

We gratefully acknowledge fruitful discussions of craniofacial reconstruction methods with Pravin Patel, MD, and Linping Zhao, PhD, both of the University of Illinois, Chicago. Thanks are due to Will Pestle for initial background discussions and to John Weinstein for photographic contributions. We are also very grateful to Robert Dakessian, Randy Walker, and Melissa Roy of Genesis Mobile Imaging, Inc. for their help in bringing a mobile CT system to the Field Museum in 2012 so that the Cap Blanc skeleton could be scanned. The 3D print of the skull was performed by the Paradigm Development Group Inc. Funding to support the project was generously provided by Joyce Chelberg.

NOTES

1. DICOM is a digital image format in which each file carries both an image and associated metadata about the object being scanned and the machinery and equipment settings used to generate the image. The format was developed in the 1980s to produce an open standard to replace the multitude of mutually incompatible proprietary medical imaging formats that were proliferating and to ensure backward compatibility. Uncompressed DICOM files (the type currently generated by most medical CT scanners) can be opened in free software such as ImageJ and also by the segmentation packages listed in the text. The DICOM standard is defined online by NEMA at http://dicom.nema.org/. See Pianykh (2008) for an accessible introduction.

2. Of the free segmentation packages mentioned earlier, only Osirix and Drishti have the capability to produce meshes. The commercial packages Amira, VG Studio Max, and Mimics all provide functionality for extracting polygon meshes from CT data stacks.

REFERENCES

Bourdier, C., A. Abgrall, O. Huard, E. Le Brun, M. Peyroux, and G. Pinçon. 2010. Histoires de bisons et de chevaux: regard sur l'évolution de la frise pariétale de Cap-Blanc (Marquay, Dordogne) à travers l'analyse du panneau de l'alcôve. *PALEO* 21: 17–38.

Brown, B. J., C. Toler-Franklin, D. Nehab, M. Burwn, D. Dobkin, A. Vlachopoulos, C. Coumas, S. Rusinkiewicz, and T. Weyrich. 2008. System for high-volume acquisition and matching of fresco fragments: reassembling Theran wall paintings. *ACM Transactions on Graphics (SIGGRAPH '08 Papers)* 27(3). 84:1–84:9.

Capitan, L. 1911. Letter, 10 August. The Field Museum Department of Anthropology Accession Files.

Capitan, L. 1914. Receipt, 30 June. The Field Museum Department of Anthropology Accession Files.

Field, H. 1938. Cap Blanc Rock Shelter. *Antiquity* 12(45): 88–9.

Gibson, I., D. Rosen, and B. Stucker. 2010. *Additive manufacturing technologies: rapid prototyping to direct digital manufacturing.* New York: Springer Science+Business Media.

Nagel, H.D. 2004. Radiation dose issues in MSCT. In *Multislice CT,* eds. M.F. Reiser et al. New York: Springer-Verlag. 24.

Schiro, M. 2011. Oddy test protocols. www.conservation-wiki.com/index.php?title=Oddy_Test_Protocols&oldid=4830 (accessed 05/06/14).

Pianykh, O. S. 2010. *Digital imaging and communications in medicine: a practical introduction and survival guide.* Berlin: Springer.

Prokop, M. 2003. Optimization of scanning technique. In *Spiral and multislice computed tomography of the body*, ed. M. Prokop et al. New York: Thieme. 109–30.

Papoint, J. 1915. Letter to M. Grimaud, 27 February. The Field Museum Department of Anthropology Accession Files.

von Bonin, G. 1935. *The Magdalenian skeleton from Cap-Blanc in the Field Museum of Natural History*. University of Illinois Medical Bulletin 32 (34) / Illinois Medical and Dental Monographs 1(1). Urbana, IL: University of Illinois.

Weiss, K. L., R. S. Cornelius, A. L. Greeley, D. Sun, I-Y, J. Chang, W. O. Boyce, and J. L. Weiss. 2011. Hybrid convolution kernel: optimized CT of the head, neck, and spine. *American Journal of Roentgenology.* 196 (February): 403–6.

Zollikofer, C. P., M. S. Ponce de León, R. D. Martin, and P. Stucki. 1995. Neanderthal computer skulls. *Nature* 375(6529): 283–5.

FURTHER READING

Geary, A. 2006. Three-dimensional virtual restoration applied to polychrome sculpture. *Conservator*, 28(1): 20–34.

Grycz, C. J. 2006. Digitising rare books and manuscripts. In *Digital heritage*, *ed.* L. W. MacDonald. London: Elsevier. 33–68.

Lang, J., and A. Middleton. 2005. Radiography: theory. In *Radiography of cultural material.* 2nd ed. Eds. J. Lang and A. Middleton. Burlington, MA: Elsevier Butterworth-Heineman. 17–18.

Lalanne, G. and H. Breuil. 1911. L'abri sculpté de Cap-Blanc (Marquay, Dordogne). *L'Anthropologie* 22: 385–402.

Nicoll, W. L. 1926. Letter to Henry Field, 27 October. The Field Museum Department of Anthropology Accession Files.

SOURCES OF SOFTWARE

3-matic
Materialise
http:/biomedical.materialise.com/3-matic

Amira
FEI Visualization Sciences Group
www.vsg3d.com/amira/overview

Blender
Blender Foundation
www.blender.org

Drishti
Ajay Limaye
https://code.google.com/p/drishti-2

Geomagic
3D Systems
www.geomagic.com/en

ImageJ
National Institutes of Health
http:/imagej.nih.gov/ij

ImageVis3D
University of Utah
www.sci.utah.edu/software/imagevis3d.html

Magics
Materialise
http:/software.materialise.com/magics

MeshLab
Visual Computing Lab—ISTI—CNR
http:/meshlab.sourceforge.net

MeshMixer
Autodesk
http:/meshmixer.com

Mimics
Materialise
http:/biomedical.materialise.com/mimics

Osirix
Antoine Rosset
www.osirix-viewer.com

Voreen
University of Münster
www.voreen.org

VG Studio Max
Volume Graphics, Gmbh
www.volumegraphics.com

ZBrush
Pixologic
http:/pixologic.com

J. P. BROWN is the Regenstein conservator at The Field Museum, Chicago, IL. He has a BSc in archaeological conservation from University College Cardiff and an MS in computer science from the University of Chicago. His research encompasses environmental monitoring and control, object conservation methods, and 3D imaging and analysis of objects. He taught practical and preventive conservation at the University of Wales, Cardiff, for five years until 1993 when he moved to the United States to work on the environmental monitoring and control of historic buildings. He joined the staff of The Field Museum in 2002 and was appointed Regenstein conservator in 2009. Address: The Field Museum, 1400 S Lake Shore Drive, Chicago, IL 50505. E-mail: jpbrown@fieldmuseum.org

ROBERT D. MARTIN received his BA in zoology from Worcester College, Oxford, England, in 1964 and his DPhil in zoology (animal behavior) from the same institution in 1967. He held an ascending series of academic posts in University College London and Birkbeck College, London, before being appointed professor and director of the *Anthropologisches Institut und Museum, Universität Zürich-Irchel*, Switzerland, in 1986. In 2001, he moved to the United States to take up the position of vice president and then provost of the Field Museum, Chicago, followed by his tenure as a Watson Armor III Curator of Biological Anthropology. His primary research interests include reconstructing primate evolution, inferring divergence times in the primate tree, allometric scaling analyses with particular reference to the scaling of brain and reproduction in primates. His new book *How we do it: the evolution and future of human reproduction* was released by Basic Books on June 11, 2013. In connection with the book, he recently started a regular monthly blog with *Psychology Today*, which can be accessed at http://www.psychologytoday.com/blog/how-we-do-it. Address: as for Brown; E-mail: rmartin@fieldmuseum.org